International Journal of Automation and Computing 16(3), June 2019, 398-412
DOI: 10.1007/s11633-018-1113-3

A Hybrid Time Frequency Response and Fuzzy Decision Tree for Non-stationary Signal Analysis and Pattern Recognition

N. R. Nayak P. K. Dash R. Bisoi

Multidisciplinary Research Cell, Siksha O Anusandhan University, Khandagiri Square, Bhubaneswar 751030, India

Abstract: A Fourier kernel based time-frequency transform is a proven candidate for non-stationary signal analysis and pattern recognition because of its ability to predict time localized spectrum and global phase reference characteristics. However, it suffers from heavy computational overhead and large execution time. The paper, therefore, uses a novel fast discrete sparse S-transform (SST) suitable for extracting time frequency response to monitor non-stationary signal parameters, which can be ultimately used for disturbance detection, and their pattern classification. From the sparse S-transform matrix, some relevant features have been extracted which are used to distinguish among different non-stationary signals by a fuzzy decision tree based classifier. This algorithm is robust under noisy conditions. Various power quality as well as chirp signals have been simulated and tested with the proposed technique in noisy conditions as well. Some real time mechanical faulty signals have been collected to demonstrate the efficiency of the proposed algorithm. All the simulation results imply that the proposed technique is very much efficient.

Keywords: Non-stationary signals, sparse S-transform (SST), scaling method, fuzzy decision tree, pattern classification.

1 Introduction

During the last several years, significant research has been undertaken to develop appropriate signal processing methods for the representation, analysis and pattern recognition of non-stationary signals embedded in noise. Initial studies in non-stationary signal processing included filter banks, spectrograms, quadratic methods for the analysis of linear frequency modulated signals that occurred in radar, geophysical systems, sonar, etc. However, multi component signals which occurred in power networks, biomedical systems, speech, seismic disturbances, and many other real world problems required the use of time-frequency transforms for their processing and analysis. This is due to the fact that the time-frequency representation (TFR) of non-stationary and nonlinear signals can provide significant information regarding the frequency content of the signals over time.

TFR is a reflection of time evolving concentration of various frequency components present in a signal, giving rise to unique signatures for each class of non-stationary signal. Some of the TFR based techniques include short-time Fourier transform (STFT)[1, 2], Gabor transform[3–6], Wigner-Ville function (WDF)[7–9], Wavelet transform (WT)[10–13], Hilbert–Huang transform (HHT)[14, 15], S-transform (ST)[16–22], etc. Most of these techniques are not adequate to provide TFR for the estimation of amplitude, phase, and instantaneous frequency and accurate pattern recognition of highly nonlinear and non-stationary signals. The STFT[23] suffers from fixed window size, while HHT[24, 25] has problems of cross-term interferences between frequency components. On the other hand, the WT[26] decomposes a signal into several time-frequency levels using dilation and translation principles which are suitable for transient analysis of time varying signals, but its performance degrades with the presence of noise in the signal and the approximation of the filter banks. Due to these factors, WT cannot estimate instantaneous frequency accurately and requires de-noising before processing.

The well known S-transform is a proven candidate for non-stationary signal analysis and pattern recognition because of its ability to predict time localized spectrum and global phase reference characteristics. Furthermore, an increased time resolution and energy concentration of ST can be achieved by a modified Gaussian window with new scalable parameters. Specifically, the ST has gained special attention due to its Fourier kernel and absolute phase reference. The reference to Fourier basis in ST enables direct interpretation of spectral component variation standards, and this property is the prime advantage of ST from the perspective of measurement of parameters and estimation, and pattern recognition. Although the

Research Article
Manuscript received July 8, 2017; accepted December 4, 2017; published online April 12, 2018
Recommended by Associate Editor Jyh-Horng Chou

conventional S-transform technique can be used for signal estimation purposes, it is computationally complex and takes long time for estimation and therefore is not suitable for real-time applications. Using the information regarding the studied system, the transform can be made computationally efficient with the help of some of the recently proposed techniques[27–31] and combining them with various frequency scaling approaches. Also, the hardware computations can be speeded up by efficiently utilizing the pre-calculated values. Thus, in this paper, the authors have proposed a fast discrete matrix based sparse S-transform (SST)[28] with complex sinusoid modulated Gaussian atom, and new frequency scaling techniques. This time-frequency transform results in drastic reduction of complexity with accurate TFR. The SST is evaluated only at the significant frequencies reducing the computations.

The sparsity is further achieved with a band pass filtering which in turn reduces the computations.

To demonstrate the effectiveness and usefulness of the proposed methodology, it is applied to 1) non-stationary power network disturbance signals, 2) non-stationary simulated chirp signals with a high-level of noise and 3) real time mechanical vibration signal with different types of faults. In power networks the short duration transients and impulsive transients may cause restarting of the computers resulting in interruption and data loss. The presence of harmonic components due to power electronics and solid state devices beyond the allowed threshold results in increased heating loss in distribution networks. The sudden multi fold increase in voltage due to impulsive transients can damage sensitive electronic equipment. The capacitive transients may cause false tripping of protective relays causing stress in the power system. Another non-stationary signal for concern is the one produced by induction motors which are used extensively in industries as variable speed drives. Half of the electricity consumed by the industry in the USA is used by the induction motors and thus a quick and accurate technique to detect and classify the induction motor faults is needed.

After the relevant features are extracted by processing the non-stationary signals by using SST, the next step is to classify the signal patterns. Although there are several linear and nonlinear classifiers, neural networks (NN)[26, 10], and support vector machines (SVM)[13, 32, 33] are the two most sought after pattern classification techniques. Several variants of neural networks like the multilayer perceptrons (MLPs)[11], radial basis function neural networks (RBFNNs), probabilistic neural networks (PNN) are widely used in a variety of applications in signal processing, power quality events recognition, image recognition, bioinformatics, etc. due to their simple structure, function approximation, and classification capabilities. However, they suffer from slower convergence speed, local minima, over fitting and generalization problems producing not very accurate classification. On the other hand, SVM is a very efficient classifier that minimizes classification error and maximizes the margin by introducing a separate hyperplane to determine the classes of data. But, it suffers from scalability problem, computational complexity, slow speed and high memory requirements for large scale problems. It is well known in the classification literature that fuzzy logic systems[18–21, 27, 29, 34–43] fused with decision trees enable one to combine uncertainty handling and approximate reasoning capabilities of fuzzy logic with ease of understanding and applicability of decision tree to provide robust classifier with strong noise immunity for a number of practical applications. Furthermore, using a data mining approach to assign certainty factor and confidence values to each fuzzy rule, the fuzzy decision tree based classifier system provides a very accurate classification system for non-stationary signals. Thus, in this paper, a fuzzy decision based classifier selects the most significant and distinguishable feature set.

The paper is organized in six sections. Apart from introduction in Section 1, the formulation of SST is presented in Section 2, where the various scaling schemes to reduce computation are outlined. Section 3 presents various simulation results of different types of non-stationary signals. Section 4 presents classification of different non-stationary signals with fuzzy decision based classifier. Section 5 presents the performance of the classifier. Concluding remarks are presented in Section 6.

2 Frequency scaled sparse S-transform (SST) formulation

A suitable frequency scaling scheme is used to form a frequency stack that contains only the significant frequency components of the signal and the discrete ST is evaluated only at these frequency components by using the well known Fourier transform algorithm (FFT) algorithm. This process reduces substantially the computational overhead for the estimation of the spectral amplitude and phase of the signal and the evolved ST will be sparse and is termed as SST[27, 28]. Furthermore, the band pass filtering is used to improve the sparsity that results in reduction of computations. Thus by reducing the numerical computations the SST will be suitable for implementing real-time instrumentation and pattern recognition events in a hardware environment.

The discrete S-transform (DST) of a signal $x(k)$ of N samples in the discrete domain is obtained as

$$S(n,j) = \sum_{k=0}^{N-1} x(k) \times W((j-k)T, \frac{n}{NT}) \exp(-\frac{i2\pi kn}{N}) \tag{1}$$

where $w(\cdot)$ is the window function. $j = 1, 2, \cdots, N$ are time indices, T is sampling time, and $n = 1, 2, \cdots, \frac{N}{2}$ are frequency indices. The frequency dependant Gaussian window function with new scalable parameters in discrete

domain is defined as

$$W(jT,\ \frac{n}{NT}) = \frac{\left(p + q\left|\frac{n}{NT}\right|^{c}\right)}{(\alpha\sqrt{2\pi})} \times WI \tag{2}$$

$$WI = \exp\left(\frac{-(jT)^2\left(p + q\left|\frac{n}{NT}\right|^{c}\right)^2}{2\alpha^2}\right) \tag{3}$$

where α and q are the scaling parameters and p, c are positive constants. The parameter c is chosen as $0 < c < 1$ to obtain damped hidden frequencies in the signal. Also an increase in value of α improves the frequency resolution and its value is chosen to lie between $0.2 < \alpha < 3$. For SST evaluation, different frequency sampling schemes such as dyadic, harmonic or automatic scaling can be chosen for those frequency components present in the frequency stack mentioned earlier. Such a scheme removes the retrieval of the unwanted and redundant information, thereby, limiting the computational requirements.

2.1 Frequency scaling schemes

The original discrete ST follows a linear frequency scaling where frequency index $n = 1,\ 2,\ \cdots,\ \frac{N}{2}$. So the ST matrix is computed for all the $\frac{N}{2}$ frequency samples. The SST is based on limiting the number of frequency samples for evaluation and thereby reducing the computations. Hence, appropriate choice of the frequency scaling is a deciding factor for the fast computation of the algorithm. This paper explores various types of frequency segmentations and proposes three novel frequency partitioning schemes.

The procedure for calculating SST in the Frequency domain:

Step 1. Transform signal samples $x(k)$, $k = 1,\ 2,\ \cdots,\ N$ to the Fourier domain $X(k)$ by fast Fourier transform algorithm (FFT) as

$$X(n) = \sum_{k=0}^{N-1} x(k)\exp(-\frac{2\pi ink}{N}). \tag{4}$$

Step 2. Formulate a data matrix $D(m,\ n)$ by convolving the elements of the FFT of the data samples $X(n)$. Where the frequency index is $m = 1,\ 2,\ \cdots, M$ and $n = 1,\ 2,\ \cdots, N$. Furthermore, according to Nyquist theorem $M = \frac{N}{2}$.

Step 3. A Gaussian window matrix in frequency domain for each set of N samples is formed. This is a two dimensional window for acquiring localization in both time and frequency domains.

$$C(m,n) = \exp(-\frac{2\pi^2(n-1)^2\alpha^2 m}{K^2}) + \exp(-\frac{2\pi^2\alpha^2(N-n+1)^2 m}{K^2}) \tag{5}$$

where m is the signal frequency and

$$K = (p + q \times m^{c}) \tag{6}$$

and α is a window factor to be chosen appropriately.

Step 4. A scaling matrix $G(m,\ n)$ based on an intelligent selection of dominant frequency components present in the signal is then formulated. This, however, depends on frequency partitioning and filtering. For each of the scaling scheme the following formulations are used:

1) Dyadic scaling

The frequency samples in dyadic scaling are chosen at an interval of $n = \left\{2^0, 2^1, 2^2 \cdots 2^l\right\}$, $2^l \le N$. The dyadic frequency scaling may skip some of the significant frequency components present and is not ideal for power signal analysis.

$G(m,\ n) = \left\{1, m \in \left(1,\ 2,\ 4, \cdots, \frac{N}{2}\right)\right\}$, otherwise, $G(m,\ n) = 0$.

2) Harmonic scaling

It is well known that most of the power quality, and mechanical vibration signals contain fundamental and harmonic frequencies. For harmonic scaling, the frequency samples in non-stationary signal analysis are chosen to include only the fundamental and harmonic frequency components, instead of evaluating SST at all the frequencies. Thus

$$G(m,\ n) = 1,\ m \in (f,\ 3f,\ 5f, \cdots, hf)$$
$$h = \text{oddnumber},\ \text{otherwise}\ G(m,n) = 0.$$

Furthermore, as there can be a small deviation in the fundamental frequency, the scaling includes frequency samples corresponding to bands of ± 5 Hz around the fundamental and harmonic frequencies. However, as presented in Table 1 automatic scaling can be used where the frequency components with significant magnitudes can be retained in the SST matrix.

3) Automatic scaling

Another scheme for frequency scaling is proposed where only those frequencies are included that have significant contribution to the spectral components of the signal. The significant frequency components can be identified from the Fourier spectrum of the signal by a threshold method. Also, the automatic scaling reduces the computations significantly where higher order harmonic components are not present.

$G(m,\ n) = 1$ for all $m \in \{\psi_m < \psi_{th}\}$, otherwise, $G(m,n) = 0$ where an intelligent scheme is used to obtain the threshold value of ψ_{th} depending on the cutoff magnitude of the frequency component used for computation.

Step 5. Multiply the data matrix $D(m,\ n)$ with the

scaling matrix $G(m, n)$ element wise to obtain

$$G' = D \circ G \tag{7}$$

where $\circ$ denotes the Hadamard product (element-by element multiplication) of the matrices.

Step 6. The window matrix C obtained in Step 3 is multiplied with the G' matrix element-wise to acquire the windowed frequency domain information to obtain $H(m, n') = G' \circ C$

where

$$H_{M\times N} = \begin{bmatrix} h(f_1,\ t_1) & \cdots & h(f_1,\ t_n) & \cdots & h(f_1,\ t_N) \\ \cdots & \cdots & \cdots & \cdots & \cdots \\ h(f_m,\ t_1) & \cdots & h(f_m,\ t_n) & \cdots & h(f_m,\ t_N) \\ \cdots & \cdots & \cdots & \cdots & \cdots \\ h(f_M,\ t_1) & \cdots & h(f_M,\ t_n) & \cdots & h(f_M,\ t_N) \end{bmatrix} \tag{8}$$

and F stands for scaled frequencies $f_1, f_2, \cdots, f_M$.

Step 7. Apply one-dimensional inverse Fourier transform along each row of $H(m,\ n')$ to obtain the SST as

$$SST(m, n) = \frac{2}{N} \sum_{k=0}^{N-1} H(m, k) \exp(\frac{2\pi nk}{N}) \tag{9}$$

and

$$SST_{M\times N} = \begin{bmatrix} s(f_1,\ t_1) & \cdots & s(f_1,\ t_n) & \cdots & s(f_1,\ t_N) \\ \cdots & \cdots & \cdots & \cdots & \cdots \\ s(f_m,\ t_1) & \cdots & s(f_m,\ t_n) & \cdots & s(f_m,\ t_N) \\ \cdots & \cdots & \cdots & \cdots & \cdots \\ s(f_M,\ t_1) & \cdots & s(f_M,\ t_n) & \cdots & s(f_M,\ t_N) \end{bmatrix}. \tag{10}$$

The important issue is proper selection of generalized Gaussian window parameters. Authors have proposed a technique for enhancing TFR energy distribution according to a performance measure (PM) at any frequency index m obtained from (5) and (6). The optimization of this PM reassigns energy concentration of the TFR.

$$PM_{[\alpha,\ p,\ q,\ c]}(m) = \sum_{n=0}^{N} \left(\frac{1}{SST_{[\alpha,\ p,\ q,\ c]}(m,\ n)} \right)^{\frac{1}{4}}. \tag{11}$$

At each frequency index m:

$$[\alpha,\ p,\ q,\ c]_{\text{optimized}} = \arg\max_{[\alpha,\ p,\ q,\ c]} [PM(m)]. \tag{12}$$

To obtain the maximum value of the PM the shape of the window is varied for each analysis frequency to obtain an accurate time-frequency distribution of the energy concentration. From (12) the optimization is performed by integrating SST over the frequency domain that preserves the frequency margin of the transform without the loss of information regarding amplitudes of the spectral components. For a sinusoidal signal of normalized amplitude 1.0 per unit, the optimization yields the values of $p = 0$, $q = 1.0$, $c = 1.0$ and $\alpha = 0.9$.

The output of the SST algorithm is a complex matrix, which is sparse because of the FFT-based frequency selection. The M rows correspond to the M frequency points and the N columns correspond to the N time points. At each time and frequency point, the signal of that particular frequency is represented by an instantaneous phasor. The multiplication of the Gaussian window for obtaining time information is done with only a few of the M values provided by the FFT operation. Rest of the rows in SST matrix are assigned zero. The various atomic operations performed for obtaining the SST of a signal using Radix-R FFT and IFFT are summarized in Table 1.

Here, in Table 1 K_H and K_A represent the odd harmonic frequencies and the number of frequencies with their amplitudes crossing the cutoff amplitude, respectively. Using the Nyquist sampling rate restriction, the value of K_H is $\leq \left(\frac{N_s}{2}\right)$, where N_s is the number of samples per fundamental cycle. Also $K_A \ll \left(\frac{N}{2}\right)$ for non-stationary signals and the fundamental signal dominates other frequencies. The SST operates on N samples at a time and therefore is represented as

$$[SST_i]_{M\times N} = SST\left(\left[x_{(i+1)},\ x_{(i+2)},\ x_{(i+3)} \cdots x_{(i+N-1)},\ x_{(i+N)}\right]\right). \tag{13}$$

Further the SST algorithm yields both time varying amplitude and phase on a sample to sample basis.

The SST output is represented as

Table 1 Atomic math operations performed in ST and SST when Radix-R FFT and IFFT are used

Method	Number of additions	Number of multiplications
General S-transform	$N \times (N+2) \times \frac{\log_R(N)}{2}$	$N \times \frac{2 \times N + \log_R(N) \times (1+N)}{2}$
SST with dyadic scaling	$N \times \log_R(N) \times \log_2\left(\frac{N}{2}\right)$	$\left(N \times \frac{\log_R(N)}{2} + N\right) \times \log_2\left(\frac{N}{2}\right)$
SST with harmonic scaling	$N \times \log_R(N) \times K_H$	$\left(N \times \frac{\log_R(N)}{2} + N\right) \times K_H$
SST with automatic scaling	$N \times \log_R(N) \times (1+K_A)$	$\left(N \times \frac{\log_R(N)}{2} + N\right) \times K_A$

$$SST(m,\ n) = A(m,\ n)\exp(j\theta(m,\ n)) \tag{14}$$

where the amplitude of the SST spectrum =

$$A(m,n) = \sqrt{\text{real}([SST(m,\ n)])^2 + \text{imag}([SST(m,\ n)])^2} \tag{15}$$

at a given frequency m and time index n. The phase angle of the SST spectrum is obtained in a similar way as

$$\theta\,(m,n) = \arctan\left(\frac{\text{Im}\,[SST\,(m,n)]}{\text{Re}\,[SST\,(m,n)]}\right). \tag{16}$$

While calculating the amplitude and phase of a particular frequency component from the SST matrix comprising of M rows, M–1 rows will have very small amplitude and hence are neglected. For a signal having frequency f its actual phase is obtained as

$$\theta_{\text{actual}}(m,n) = \theta(m,n) - \frac{2\pi f}{f_s} \tag{17}$$

where f_s the sampling rate is in hertz and the phase is represented in radians.

For obtaining the fundamental amplitude and phase angle at the sample number t

$$A_1(t) = \sqrt{(\text{real}[s(f_1,\ t)])^2 + (\text{imag}[s(f_1,\ t)])^2} \tag{18}$$

$$\varphi_1(t) = \tan^{-1}\left\{\frac{(\text{imag}[s(f_1,t)])}{(\text{real}[s(f_1,t)])}\right\}. \tag{19}$$

By definition the instantaneous fundamental angular frequency is obtained as

$$f_1 = \frac{\mathrm{d}\varphi_1}{\mathrm{d}t} = \frac{SH_R \times \frac{\mathrm{d}(SH_I)}{\mathrm{d}t} - SH_I \times \frac{\mathrm{d}(SH_R)}{\mathrm{d}t}}{(SH_R)^2 + (SH_I)^2} \tag{20}$$

where

$$SH_R = \text{real}[s(f_1,\ t)],\ SH_I = \text{imag}[s(f_1,\ t)] \tag{21}$$

and the actual phase is obtained as

$$\theta_{1\text{true}} = \theta_1(t) - 2(\frac{f}{f_s})\pi. \tag{22}$$

For the estimation of harmonics following equations are used:

$$A_m(t) = \sqrt{(\text{real}[s(f_m,\ t)])^2 + (\text{imag}[s(f_m,\ t)])^2} \tag{23}$$

$$\theta_m(t) = \tan^{-1}\left\{\frac{(\text{imag}[s(f_m,t)])}{(\text{real}[s(f_m,t)])}\right\} \tag{24}$$

$$\theta_{m\,\text{corrected}} = \theta_m(t) - 2\left(\frac{f_m}{f_s}\right)\pi. \tag{25}$$

In the presence of noise in the signal, the linear property of both the S transform, and SST ensure that SST (noisy signal) = SST(signal without noise) + SST(noise).

Thus a simple threshold can be used to remove the noise from the signal. However, for numerical experimentation white Gaussian noise is added to the simulated non-stationary signals to test the efficacy of SST and proposed fuzzy logic based classifier.

3 Computer simulation results

The proposed formulation is tested on different types of non-stationary signals such as mechanical vibration signal, chirp signal and power quality disturbance signal, etc. The following case studies are attempted in this paper.

Case 1. Power quality disturbance signals

In recent years power quality (PQ) disturbances like voltage sags and swells, harmonics due to power-electronics controlled loads, voltage spikes and notches due to converters and inverter operations, voltage flicker, capacitor switching transients, and lightning discharges, etc. can cause immense damages to electrical utilities in terms of production loss and increase in cost for replacing the damaged equipment. Thus for supplying good quality electric power of correct voltage, frequency, absence of waveform distortions, it is customary to detect and classify these PQ disturbance events accurately[44] using power quality monitoring instruments. Some important power quality disturbance patterns are taken in this paper to illustrate the efficacy of the proposed sparse time frequency transform. Also suitable mitigating action can be initiated to improve power supply quality to customers, and maintain the performance of industrial or commercial organizations at desired levels.

Some of the power quality signals with frequently occurring disturbances, such as oscillatory transient (A1), voltage sag (A2), and flicker (A3), etc., have been simulated in Matlab. All the signals are corrupted with 20 dB noise, which is quite large for power network noise contamination. The frequency contours are obtained by SST with modified Gaussian window. Time localized frequency information is obtained from the contours. Figs. 1(a)–(b), 2(a)–(b) and 3(a)–(b) illustrate the frequency content and amplitude phase plot of the test patterns of power quality. The low frequency component in Fig. 2(a) provides the fundamental frequency of voltage sag. Frequency contours of oscillatory transient and flicker in Figs. 1(a) and 3(a) show high frequency components.

Case 2. Mechanical vibration signal

In most of the industries induction motors are used as preferred drives and the conditions of these motors should

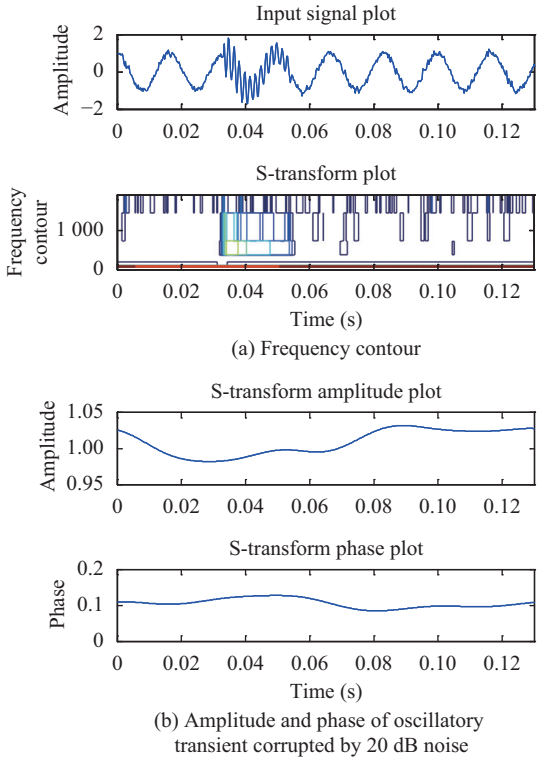

Fig. 1 (a) Frequency contour and (b) amplitude and phase of oscillatory transient corrupted by 20 dB noise are obtained through SST with modified Gaussian window

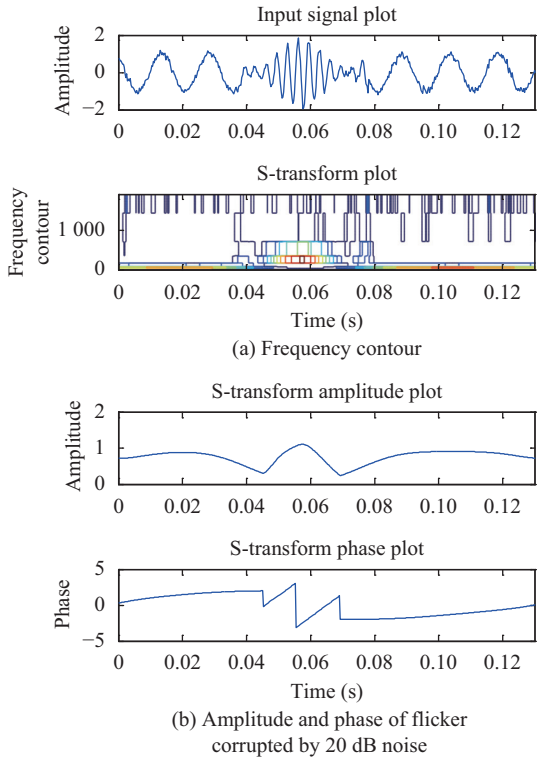

Fig. 3 (a) Frequency contour and (b) amplitude and phase of flicker corrupted by 20 dB noise are obtained through SST with modified Gaussian window

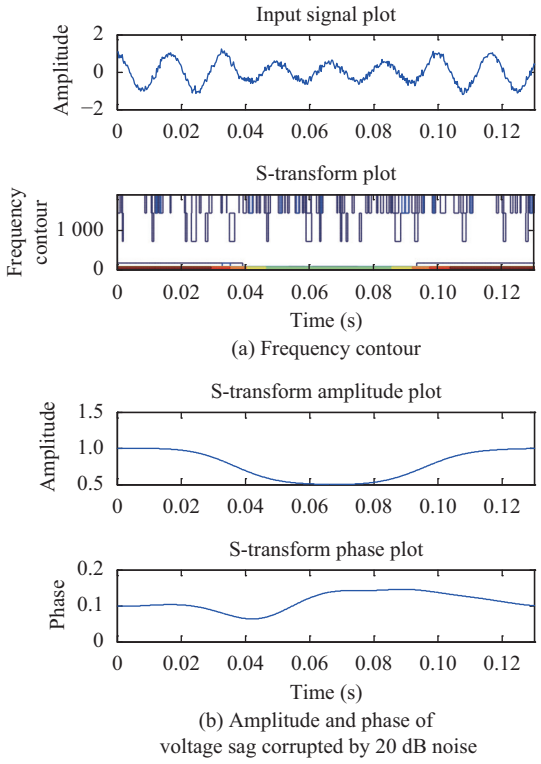

Fig. 2 (a) Frequency contour and (b) amplitude and phase of voltage sag corrupted by 20 dB noise are obtained through SST with modified Gaussian window

be monitored to detect faults and other disturbances. Half of the electricity consumed by the industry in USA is used by the induction motors. For anticipating work stoppage, a fast and accurate method is necessary to detect and classify different types of faults. Two types of mechanical faults like the misalignment (M2) and bowed rotor (M3) along with the healthy (M1) signal are considered in this paper for analysis and pattern recognition. Misalignment fault is basically machine components deterioration that occurs when two machines are coupled. Bowed rotor is a serious defect of rotating systems. These defects sometimes developed on a motor that has been allowed to remain idle for a long time. While remaining idle the weight of the rotor causes the shaft to deflect. For this study experimental data is obtained from the mechanical laboratory by generating signals for different load conditions, faults, and other types of disturbances, etc. Collected mechanical signal waveforms corrupted by misalignment and bowed rotor are processed using the SST algorithm with modified Gaussian window to get the time frequency contours. Figs. 4(a)–(b), 5(a)–(b) and 6(a)–(b) show the time frequency contours along with the amplitude and phase plot of the healthy signal, bowed rotor and misalignment cases, respectively. From the figures it can be seen that the patterns of the frequency contours are all distinguishable from each other.

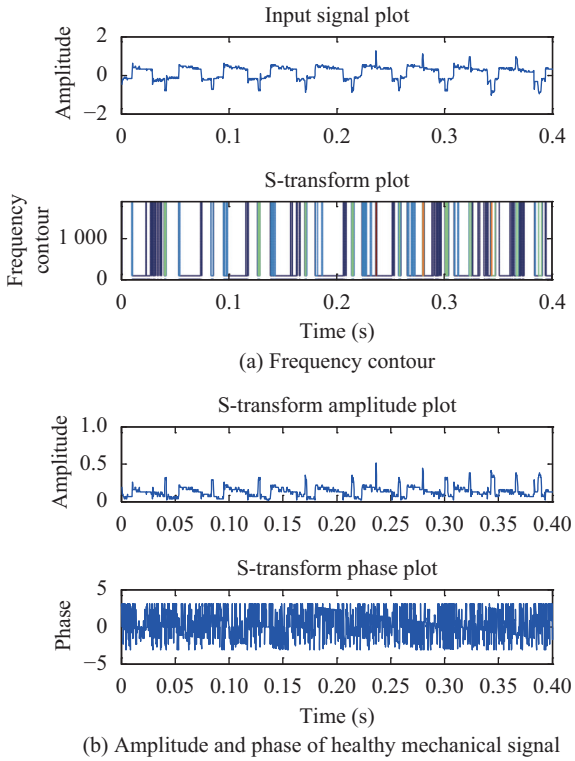

Fig. 4 (a) Frequency contour and (b) amplitude and phase of healthy mechanical signal are obtained through SST with modified Gaussian window

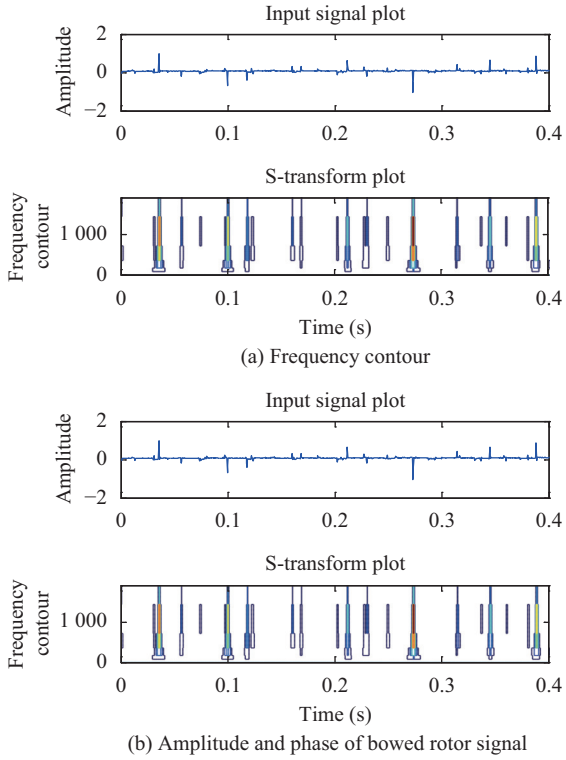

Fig. 5 (a) Frequency contour and (b) amplitude and phase of bowed rotor signal are obtained through SST with modified Gaussian window

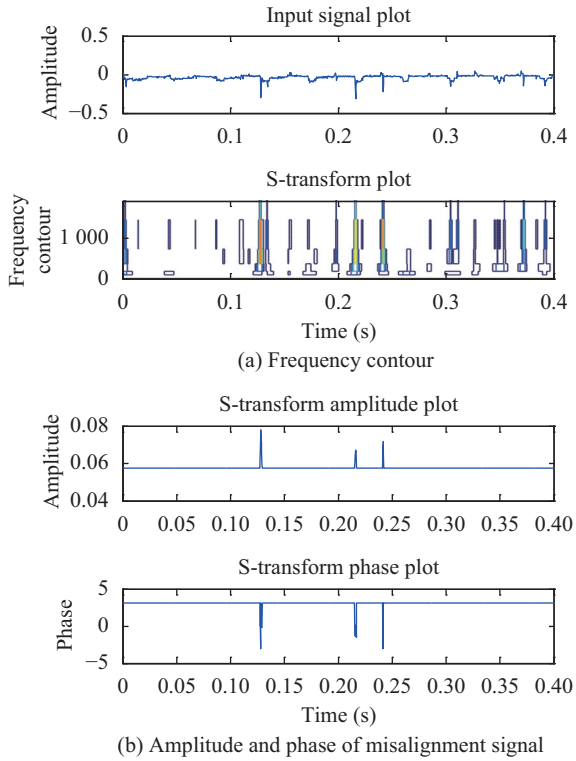

Fig. 6 (a) Frequency contour and (b) amplitude and phase of misalignment signal are obtained through SST with modified Gaussian window

Case 3. Chirp signals

Chirp signals are everywhere in nature. They are developed from many audio signals such as speech, bird song, music etc. Different man made systems also develop chirp signals. They are used in different engineering applications such as echo location systems (radar, sonar), passive sensor array systems, communication systems, mechanics and vibrations etc. In biomedical systems also different types of chirps occur. Time frequency transforms are very useful to analyze different types of chirp signals. In this paper three different types of basic chirp signals, linear (C1), power law (C2) and hyperbolic (C3) are synthesized and tested with this SST algorithm. Figs. 7(a)–(b), 8(a)–(b) and 9(a)–(b) show the frequency contours, amplitude, and phase plot of different chirp signals; linear chirp, power law and hyperbolic chirp, etc. From all the figures it can be observed that with the continuous frequency change, the frequency contours are also changing. The high frequency as well as low frequency range of different types of chirps can be distinguished easily from the frequency contours obtained using SST. All the mathematical models of synthesized signals are given in Table 2.

3.1 Feature extraction

After obtaining the spectral characteristics of the disturbance signals, it is necessary to extract some relevant

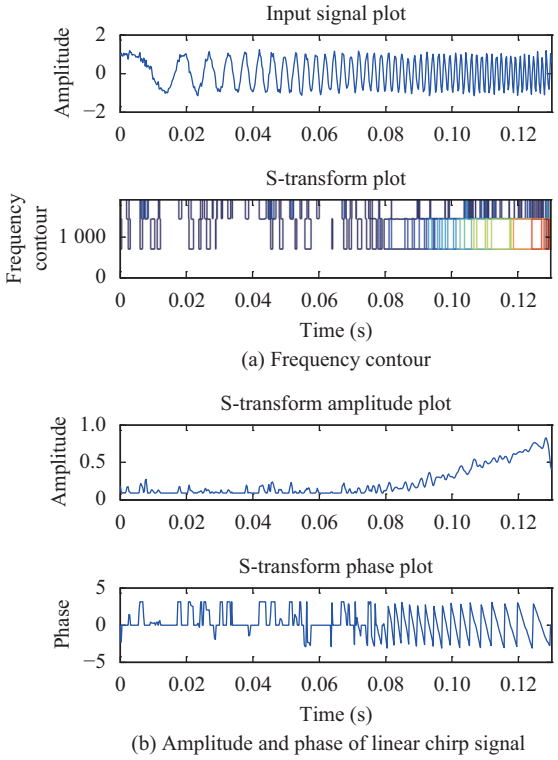

(a) Frequency contour

(b) Amplitude and phase of linear chirp signal

Fig. 7 (a) Frequency contour and (b) amplitude and phase of linear chirp signal are obtained through SST with modified Gaussian window

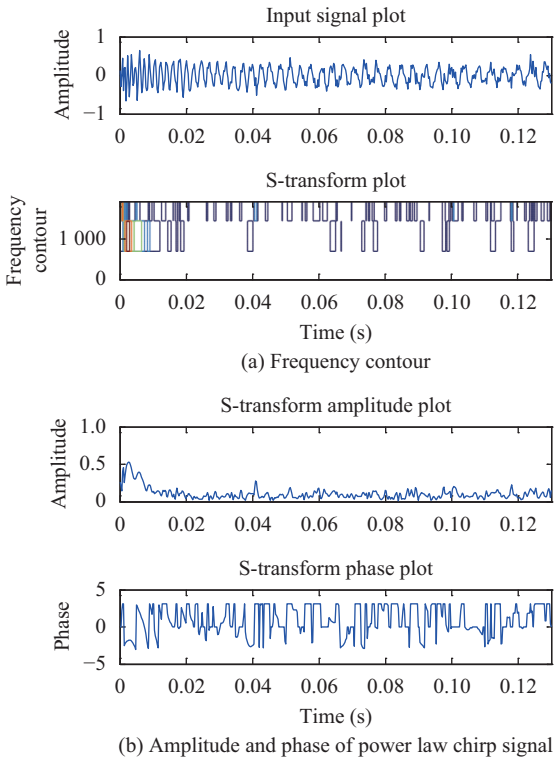

(a) Frequency contour

(b) Amplitude and phase of power law chirp signal

Fig. 8 (a) Frequency contour and (b) amplitude and phase of power law chirp signal are obtained through SST with modified Gaussian window

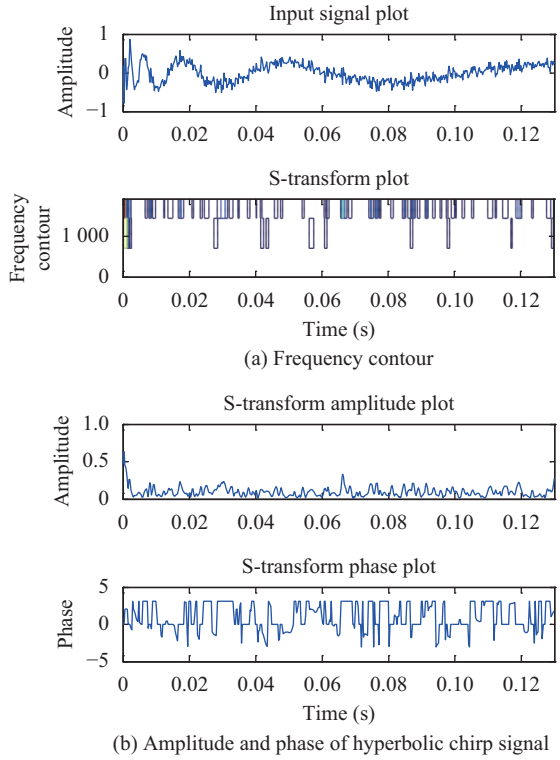

(a) Frequency contour

(b) Amplitude and phase of hyperbolic chirp signal

Fig. 9 (a) Frequency contour and (b) amplitude and phase of hyperbolic chirp signal are obtained through SST with modified Gaussian window

features from the time-frequency contours to detect and classify the type of the disturbances. The effectiveness of a classifier is directly influenced by the accurate feature selection. Different groups of disturbance data can be discriminated with the choice of proper features. The five most significant features for signal pattern classification are derived from the SST and defined as follows:

Energy of the signal (F_1).

For SST analysis, with samples with $n = 1, 2, 3, \cdots, N$, where N is the total number of samples.

Its cumulative spectral energy (F_1) is obtained using (9) and is defined as

$$\text{Energy} = F_1 = \sum_{m=1}^{M} [\max(\text{abs}(SST(m,\ n)))]^2 \quad n = 1,\ 2,\ 3, \cdots, N. \tag{26}$$

Minimum amplitude of the signal (F_2).

$$F_2 = \min(\max(\text{abs}(SST(m,\ n)))). \tag{27}$$

Standard deviation (F_3).

The standard deviation is a measure of how the data has been spread out.

$$F_3 = \sqrt{\frac{1}{M}\sum_{m=1}^{M}([\max(\text{abs}(\text{SST}(m,n)))] - \hat{x}_\mu)^2} \quad n = 1,\ 2,\ 3, \cdots, N \tag{28}$$

Table 2 Non-stationary signal models with disturbances

Non-stationary signals	Event	Equation	Parameters variation
Normal		$H(t)=\sin(w_b t)+n_l$	$w_b=2\times\pi\times 60$ rad/s
Sag	A1	$H(t)=\left[1-\alpha\begin{pmatrix}U(t-t_1)\\ -U(t-t_2)\end{pmatrix}\right]\sin(w_b t)+n_l$	$0.1\le\alpha\le 0.9$ $\mathrm{T}\le t_2-t_1\le 8\,\mathrm{T}$
Flicker	A2	$H(t)=[1+\alpha\sin(2\times\pi\times\beta\times t)]\sin(w_b t)+n_l$	$0.1\le\alpha\le 0.2$ $10\,\mathrm{Hz}\le\beta\le 20\,\mathrm{Hz}$
Oscillatory transient	A3	$H(t)=\sin(w_b t)+\alpha\exp(-\frac{(t-t_1)}{\tau})$ $(U(t-t_1)-U(t-t_2))$ $\sin(2\times\pi\times f_n\times t)+n_l$	$0.2\le\alpha\le 0.8$ $0.5\,\mathrm{T}\le(t_2-t_1)\le 2\,\mathrm{T}$ $400\,\mathrm{Hz}\le fn\le 800\,\mathrm{Hz}$ $10\,\mathrm{ms}\le\tau\le 40\,\mathrm{ms}$
		Chirp signals: $x(t)=A(t)\exp\{i\Phi(t)\}$	
Linear chirp	C1	$A(t)\ \alpha\ \exp\{-\pi\gamma t^2\}$ $\Phi(t)\ \alpha\ 2\pi\left(\frac{\xi t^2}{2}+\beta t\right)$	$0.9\ge\xi\ge 0.1$ $0.5\ge\beta\ge 0.01$ $1\ge\gamma\ge 0$
Power law chirp	C2	$A(t)\ \alpha\ t^{-\xi}$ $\Phi(t)\ \alpha\ 2\pi\mathrm{d}t^{\beta}$	$0.9\ge\xi\ge 0.1$ $0.5\ge\beta\ge 0.01$
Hyperbolic chirp	C3	$A(t)\ \alpha\ t^{-\xi}$ $\Phi(t)\ \alpha\ 2\pi\mathrm{d}\log(t)$	$0.9\ge\xi\ge 0.1$

where

$$\hat{x}_{\mu}=\mathrm{mean}(\max(\mathrm{abs}(SST(m,\ n)))). \tag{29}$$

If a data set looks same on the left and right of the centre point, then the measure of this symmetry is known as skewness.

$$F_4=\frac{\sum_{m=1}^{M}([\max(\mathrm{abs}(SST(m,\ n)))]-\hat{x})^3}{(M-1)\,F_3^3}. \tag{30}$$

Kurtosis (F_5).

Kurtosis is a measure of whether the SST output set has high or small number of peaks relative to a normal distribution.

$$F_5=\frac{\sum_{m=1}^{M}([\max(\mathrm{abs}(SST(m,n)))]-\hat{x})^4}{(M-1)\,F_3^4}. \tag{31}$$

4 Classification of non-stationary signals

For non-stationary signals corrupted by 20 dB noise and different types of fault are classified with fuzzy decision tree classifier. In case of mechanical disturbances, healthy signal can be easily classified from the faulty signals with a simple decision tree using the most significant features like kurtosis and skewness. But to classify other mechanical disturbances and other non-stationary signals such as power quality and chirp signals a fuzzy decision base classifier is needed.

4.1 Fuzzy decision tree (FDT) classifier

The most important feature of fuzzy decision tree[43, 45, 46] is that it breaks the complex decisions into simple ones so. It has a wide application in pattern classification. In this paper, a hard decision tree is constructed at first and subsequently the hard decision boundaries are formed using the fuzzy membership functions for the features. In case of decision tree classifier, choosing of different subsets of feature is flexible which is not available in single stage classifiers. The data sets in individual iteration are started from a root node. Then split into two child nodes, until a stopping criterion is achieved. Gini′s diversity index is utilized to obtain the fittest condition formulated at individual node. Division between events rather than node miscellany is made possible for non-stationary signal classification, using the towing rule base. This rule is particularly suitable for multiclass problems. All the classes are divided into two groups by this rule. Splits preserving the correlated prototypes are strictly chosen. For a number of mechanical faults as well as power quality problems with δ number of patterns, with the percentage of annotations of c-th pattern at n-th node defined as $p_{\delta nz}$, the Gini′s diversity index is defined as

$$G_{DI}=\sum_{c=1}^{\delta}p_{\delta n}[1-p_{\delta n}] \tag{32}$$

where G_{DI} is further vulnerable to alterations in the likelihood at each node than to the misclassification imprecision.

Further, the most significant features are needed to be selected to formulate fuzzy decision tree through which

highest classification accuracy can be obtained. In the next step, the judgment rules are fuzzified using triangular and trapezoidal membership functions to formulate the FDT.

The triangular membership function with legs s_1, s_2, s_3 and s as input, respectively, is defined as

$$\mu(s_1,\ s_2,\ s_3) = \begin{cases} 0, & \text{if } s < s_1 \\ \dfrac{(s - s_1)}{(s_2 - s_1)}, & \text{if } s_1 \le s < s_2 \\ \dfrac{(s_3 - s)}{(s_3 - s_2)}, & \text{if } s_2 \le s \le s_3 \\ 0, & \text{if } s_3 < s. \end{cases} \tag{33}$$

The trapezoidal membership function with legs s_1, s_2, s_3, s_4 and s as input, respectively, is defined as

$$\mu(s_1,\ s_2,\ s_3,\ s_4) = \begin{cases} 0, & \text{if } s < s_1 \\ \dfrac{(s_1 - s)}{(s_2 - s_1)}, & \text{if } s_1 \le s < s_2 \\ 1, & \text{if } s_{2,3,4} \le s. \end{cases} \tag{34}$$

The membership functions for various fuzzy sets of the features F_1 – F_5 have been illustrated in Figs. 10 to 12. The detailed value of the membership points of the triangular and trapezoidal membership functions are mentioned in Table 3 for power quality; Table 4 is for chirp signal and Table 5 is for mechanical fault.

For deriving association rules with antecedents "A" and consequents "C" of the "α" assessment rules is very much significant for the application of certainty factor based on support and confidence indices. The support (S) of a particular rule "α-th" is an indication of the number of instances the consequents (C) and the antecedents (A) occur simultaneously and mathematically defined as

$$S(A \to C) = p(A \cap C) = \frac{\sum\limits_{a \in b} \mu_{A_i}(X_a)}{b} \tag{35}$$

where "a" is the number of attributes (X) for classification and "i" is the number of membership functions, respectively.

In a similar manner, the confidence i.e., certainty factor (CF) of a particular rule "α" is an indication of the probability that the consequents (C) strictly follow the respective antecedents (A) of the assessment rules, and mathematically defined as

$$CF(A \to C) = \frac{p(A \cap C)}{p(A)} = \frac{\sum\limits_{a \in b} \mu_{A_i}(X_a)}{\sum\limits_{a=1}^{b} \mu_{A_i}(X_a)}. \tag{36}$$

Finally, the certainty factor (K_F) for particular rule "α" is defined as

$$K_F = CF(A \to C) - \rho \tag{37}$$

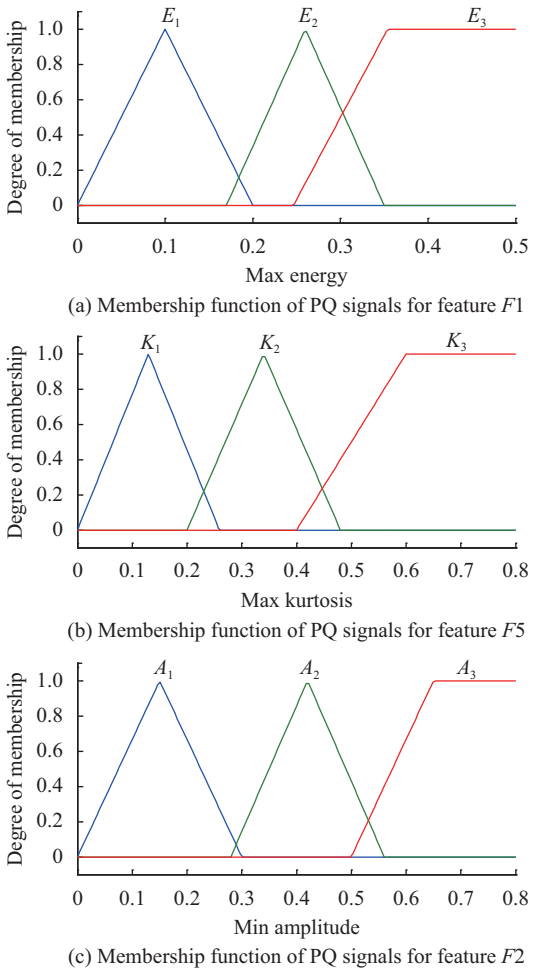

(a) Membership function of PQ signals for feature $F1$

(b) Membership function of PQ signals for feature $F5$

(c) Membership function of PQ signals for feature $F2$

Fig. 10 Plot showing the membership functions of PQ signals for the features (a) F_1, (b) F_5 and (c) F_2, respectively

where ρ is the average confidence value for each rule defined as

$$\rho = \frac{1}{b-1} \sum_{\substack{a=1 \\ a \ne b}}^{b} CF(A \to C). \tag{38}$$

Cross validation is a model evaluation method and it is better than residuals. In case of residual evaluations it is very difficult to say how well the trainer will do when it is required for classification or predictions with new dataset. This problem can be overcome with this cross validation technique. There are many types of cross validation methods, such as hold out method, k-fold cross validation, leave one out cross validation, etc. In this paper, hold out method has been used. It is the simplest kind of cross validation where the data set is separated into two sets, called the training set and testing set. Training of the system is done with the training data set only. The trained system has no idea of the testing data set. Before training, some of the data is removed to test the performance of the system. Using Table 2 with different paramet-

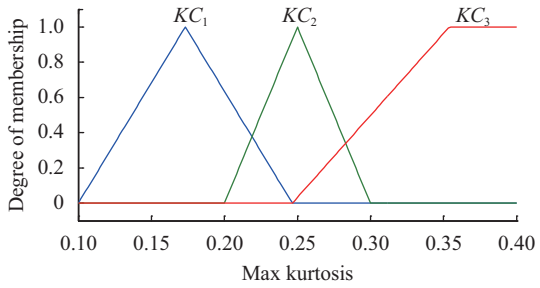

(a) Membership function of chirp signals for feature $F5$

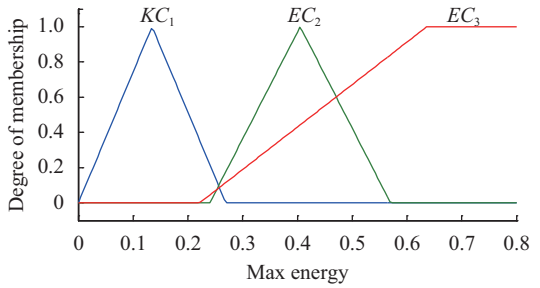

(b) Membership function of chirp signals for feature $F1$

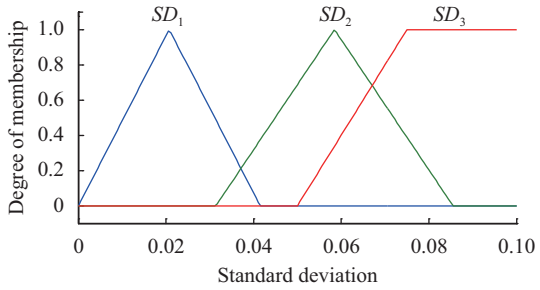

(c) Membership function of chirp signals for features $F3$

Fig. 11 Plot showing the membership functions of different chirp signals for the features (a) F_5, (b) F_1 and (c) F_3, respectively

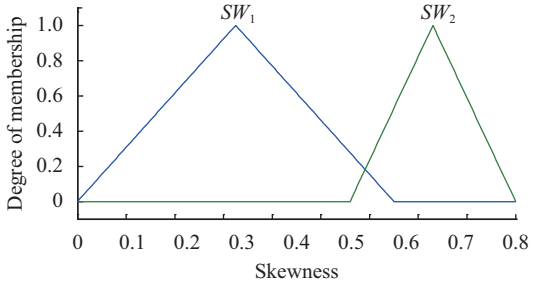

(a) Membership function of mechanical signals for feature $F4$

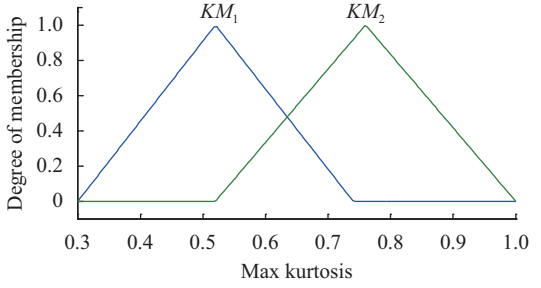

(b) Membership function of mechanical signals for feature $F5$

Fig. 12 Plot showing the membership functions of mechanical signals for the features (a) F_4 and (b) F_5, respectively

Table 3 Detailed value of the power quality membership points of the triangular and trapezoidal membership functions as shown in Fig. 10

Sl. number	Membership name	Class value	a	b	c	d
1	$\mu(F_5)K_1$	A1	0	0.1295	0.259	–
2	$\mu(F_5)K_2$	A2	0.2	0.34	0.48	–
3	$\mu(F_5)K_3$	A3	0.4	0.6	0.8	0.8
4	$\mu(F_1)E_1$	A1	0	0.1	0.2	–
5	$\mu(F_1)E_2$	A2	0.17	0.26	0.35	–
6	$\mu(F_1)E_3$	A3	0.2465	0.354	0.5	0.5
7	$\mu(F_2)A_1$	A1	0	0.15	3	–
8	$\mu(F_2)A_2$	A2	0.28	0.42	0.56	–
9	$\mu(F_2)A_3$	A3	0.5	0.65	0.8	0.8

ers, number of samples has been generated for each class. Total 1 200 samples have been used for power signals as well as chirp signals. Initial 300 samples are separated to perform cross validation. Then, 900 samples are left for training the network. In this case also 300 samples are randomly selected from the total data set for testing the performance of the proposed classifier. The mechanical signal is the real time experimental signal and in this case 25 samples are taken for testing.

4.2 Certainty factor based fuzzy rule base

The fuzzy decision rules for the FDT comprise the rule base for classification. In the next step, we associate each of the fuzzy rules with a certainty factor K_F. Table 6 shows the certainty factor based fuzzy rules formulation, firing strength calculation and decision making variable. All the fuzzy rules have been accumulated in this table for all types of non-stationary signals.

Thus the final decision rule for power quality, chirp signals and mechanical faults using FDT can be written as

Power quality:

Decision 1_{PQ} (D_{1PQ}): if $\alpha_{1PQ} > \alpha_{2PQ}$ && $\alpha_{1PQ} > \alpha_{3PQ}$ then "A1"

Decision 2_{PQ} (D_{2PQ}): if $\alpha_{2PQ} > \alpha_{1PQ}$ && $\alpha_{2PQ} > \alpha_{3PQ}$ then "A2"

Decision 3_{PQ} (D_{3PQ}): if $\alpha_{3PQ} > \alpha_{1PQ}$ && $\alpha_{3PQ} > \alpha_{2PQ}$ then "A3".

Chirp signal:

Decision 1_{CH} (D_{1CH}): if $\alpha_{1CH} > \alpha_{2CH}$ && $\alpha_{1CH} > \alpha_{3CH}$ then "C3"

Decision 2_{CH} (D_{2CH}): if $\alpha_{2CH} > \alpha_{1CH}$ && $\alpha_{2CH} > \alpha_{3CH}$ then "C2"

Table 4 Detailed value of the chirp membership points of the triangular and trapezoidal membership functions as shown in Fig. 11

Sl. number	Membership name	Class value	a	b	c	d
1	$\mu(F_1)EC_1$	C1	0	0.13465	0.2693	–
2	$\mu(F_1)EC_2$	C2	0.24	0.405	0.57	–
3	$\mu(F_1)EC_3$	C3	0.2213	0.6363	0.8	0.8
4	$\mu(F_5)KC_1$	C1	0.1	0.17325	0.2465	–
5	$\mu(F_5)KC_2$	C2	0.2	0.25	0.3	–
6	$\mu(F_5)KC_3$	C3	0.2465	0.354	0.4	0.4
7	$\mu(F_3)SD_1$	C1	0	0.02075	0.0415	–
8	$\mu(F_3)SD_2$	C2	0.0314	0.05845	0.0855	–
9	$\mu(F_3)SD_3$	C3	0.05	0.075	0.1	0.1

Table 5 Detailed value of the mechanical membership points of the triangular and trapezoidal membership functions as shown in Fig. 12

Sl. number	Membership name	Class value	a	b	c
1	$\mu(F_4)SW_1$	M2	0	0.325	0.65
2	$\mu(F_4)SW_2$	M3	0.56	0.73	0.9
3	$\mu(F_5)KM_1$	M2	0.3	0.52	0.74
4	$\mu(F_5)KM_2$	M3	0.52	0.76	1

Decision 3_{CH} (D_{3CH}): if $\alpha_{3CH} > \alpha_{1CH}$ && $\alpha_{3CH} > \alpha_{2CH}$ then "C1".

Mechanical signal:

Decision 1_M (D_{1M}): if $\alpha_{1M} > \alpha_{2M}$ && $\alpha_{1M} > \alpha_{3M}$ then "M2"

Decision 2_M (D_{2M}): if $\alpha_{2M} > \alpha_{1M}$ && $\alpha_{2M} > \alpha_{3M}$ then "M3".

Tables 7 to 9 show the certainty factors of the fuzzy rules for some randomly selected feature sets for each class of all non-stationary signals. It is significantly observed from Tables 7 to 9 that the CF of a particular rule is highest for the class which corresponds to the consequent of that particular rule.

5 Performance evaluation of the proposed classifier

The proposed method has lesser computational time and acceptable classification accuracy. To further verify the real time capability of the proposed algorithm, it was implemented on a TMS 320C6713 Starter Kit (DSK)[47] and embedded Matlab coder. TMS 320C6713 is from Texas instruments and a 32 bit floating point digital signal processor. The real time data exchange (RTDX) had been used to exchange the data between the host pc and the target DSK for analyzing the real time implementation.

To provide the interface between PC & DSK, a software tool embedded Target for TI C6000 DSP and Matlab link for code composer studio (CCS) is used by the RTDX. To demonstrate the speed of execution of the SST, the conventional ST takes around 0.0580 s for processing 10 cycles of data (64 samples per cycle), whereas the SST algorithm with dyadic scaling, and automatic scaling consumes significantly less time i.e., 0.0032 s, and 0.0055 s, respectively. Thus the speed advantage of the SST algorithm is more than 10 times. However, with a smaller cutoff magnitude of the harmonics, the speed can be easily increased to more than 30 times for the automatic scaling based SST. The performance of the pro-

Table 6 Certainty factor based fuzzy rule formation

Rule number	Rule	Certainty factor based event selection	Firing strength	Decision making variable
Rule1_{PQ}	If F_1 is E_1 && F_2 is A_2 && F_5 is K_2	"A1" with certainty factor K_{R1PQ}	$\beta_{1PQ} = (\mu(F_1)E_1, \mu(F_2)A_2, \mu(F_5)K_2)$	$\alpha_{1PQ} = \beta_{1PQ} \times K_{R1PQ}$
Rule2_{PQ}	If F_1 is E_2 && F_2 is A_1 && F_5 is K_3	"A2" with certainty factor K_{R2PQ}	$\beta_{2PQ} = (\mu(F_1)E_2, \mu(F_2)A_1, \mu(F_5)K_3)$	$\alpha_{2PQ} = \beta_{2PQ} \times K_{R2PQ}$
Rule3_{PQ}	If F_1 is E_3 && F_2 is A_3 && F_5 is K_1	"A3" with certainty factor K_{R3PQ}	$\beta_{3PQ} = (\mu(F_1)E_3, \mu(F_2)A_3, \mu(F_5)K_1)$	$\alpha_{3PQ} = \beta_{3PQ} \times K_{R3PQ}$
Rule1_{LCH}	If F_3 is SD_1 && F_1 is EC_1 && F_5 is KC_2	"C3" with certainty factor K_{R1CH}	$\beta_{1CH} = (\mu(F_1)EC_1, \mu(F_3)SD_1, \mu(F_5)KC_2)$	$\alpha_{1CH} = \beta_{1CH} \times K_{R1CH}$
Rule2_{PCH}	If F_3 is SD_2 && F_1 is EC_3&& F_5 is KC_3	"C2" with certainty factor K_{R2CH}	$\beta_{2CH} = (\mu(F_1)EC_3, \mu(F_3)SD_2, \mu(F_5)KC_3)$	$\alpha_{2CH} = \beta_{2CH} \times K_{R2CH}$
Rule3_{HCH}	If F_3 is SD_3 && F_1 is EC_2&& F_5 is KC_1	"C1" with certainty factor K_{R3CH}	$\beta_{3CH} = (\mu(F_1)EC_2, \mu(F_3)SD_3, \mu(F_5)KC_1)$	$\alpha_{3CH} = \beta_{3CH} \times K_{R3CH}$
Rule1_M	If F_4 is SW_2&& F_5 is KM_2	"M2" with certainty factor K_{R1M}	$\beta_{1M} = (\mu(F_4)\ SW_2, \mu(F_5)KM_2)$	$\alpha_{1M} = \beta_{1M} \times K_{R1M}$
Rule2_M	If F_4 is SW_1 && F_5 is KM_1	"M3" with certainty factor K_{R2M}	$\beta_{2M} = (\mu(F_1)\ SW_1, \mu(F_5)\ KM_1)$	$\alpha_{2M} = \beta_{2M} \times K_{R2M}$

Table 7 Detailed value of the certainty factors for fuzzy rules for PQ disturbances

Class	A1	A2	A3
K_{R1PQ}	0.971	0.014	0.015
K_{R2PQ}	0.021	0.951	0.028
K_{R3PQ}	0.019	0.017	0.964

Table 8 Detailed value of the certainty factors for fuzzy rules for chirp signals

Class	C1	C2	C3
K_{R1CH}	0.965	0.021	0.014
K_{R2CH}	0.019	0.956	0.025
K_{R3CH}	0.011	0.012	0.977

Table 9 Detailed value of the certainty factors for fuzzy rules for mechanical signal

Class	M2	M3
K_{R1M}	0.956	0.044
K_{R2M}	0.046	0.958

posed method is tested in noisy condition because in real life operation signals are always contaminated with noise. The general accuracy has been considered as the index to evaluate the performance of the classification algorithm.

$$\text{Accuracy}(\%) = \frac{\text{Number of detection of true events}}{\text{Number of true events}} \times 100. \quad (39)$$

The results of Tables 10 and 11 represent the confusion matrix. From Table 12, it can be observed that for various types of events, the performance of the proposed method is within the acceptable range. The classification performance of mechanical signals is given in Table 13.

Table 10 Confusion matrix for PQ events

Class	A1	A2	A3
A1	299	1	0
A2	1	299	0
A3	0	2	298

Table 11 Confusion matrix for chirp signals

Class	C1	C2	C3
C1	298	2	0
C2	1	299	0
C3	0	0	300

Table 12 Classification performance of the proposed scheme for PQ and chirp signal

Event	Accuracy (%)
A1	99.67
A2	99.67
A3	98.33
C1	98.33
C2	99.67
C3	100

Table 13 Classification performance of the proposed scheme for mechanical signal

Conditions	Number of samples	Healthy	Rotor-bar	Mis-alignment	Performance (%)
Healthy	25	25	0	0	100
Healthy	25	25	0	1	96
Mis-alignment	25	0	24	1	96

6 Conclusions

The conventional S-transform is modified in a novel way and the simplifications required to make it fast when analyzing non-stationary signals are presented. The resulting new SST is very sparse due to the adoption of frequency scaling techniques and is suitable for real time implementation. Various time varying distorted signals like the power quality disturbance signals, multi component chirp signals, and mechanical vibration signals embedded in noise are used for analysis and pattern recognition. The simulation results show that the proposed algorithm with the classifier gives an acceptable performance. The performance is acceptable also in noisy condition. The algorithm SST requires low computations and distinguishable features can be obtained from the time frequency matrix. Computations are less and therefore the algorithm processes the non-stationary signals much faster. From all the simulation results it is clear that this method is robust and can classify different types of highly nonlinear and non-stationary signals in the presence of noise and accurately classify the patterns.

References

[1] Y. C. Eldar, P. Sidorenko, D. G. Mixon, S. Barel, O. Cohen. Sparse phase retrieval from short-time Fourier measurements. *IEEE Signal Processing Letters*, vol. 22, no. 5, pp. 638–642, 2015. DOI: 10.1109/LSP.2014.2364225.

[2] L. B. Almeida. The fractional Fourier transform and time-frequency representations. *IEEE Transactions on Signal Processing*, vol. 42, no. 11, pp. 3084–3091, 1994. DOI: 10.1109/78.330368.

[3] A. R. Abdullah, A. Z. Sha'ameri, M. S. Norhashimah. Power quality analysis using spectrogram and gabor transformation. In *Proceedings of Asia-Pacific Conference on*

Applied Electromagnetics, IEEE, Melaka, Malaysia, pp. 1–5, 2007. DOI: 10.1109/APACE.2007.4603964.

[4] S. H. Cho, G. Jang, S. H. Kwon. Time-frequency analysis of power-quality disturbances via the Gabor–Wigner transform. *IEEE Transactions on Power Delivery*, vol. 25, no. 1, pp. 494–499, 2010. DOI: 10.1109/TPWRD.2009.2034832.

[5] S. J. Huang, C. L. Huang, C. T. Hsieh. Application of Gabor transform technique to supervise power system transient harmonics. *IEE Proceedings-Generation, Transmission and Distribution*, vol. 143, no. 5, pp. 461–466, 1996. DOI: 10.1049/ip-gtd:19960534.

[6] L. Tao, S. Z. Yan, W. Zhang. Time-frequency analysis of nonstationary vibration signals for deployable structures by using the constant-Q nonstationary gabor transform. *Mechanical Systems and Signal Processing*, vol. 75, pp. 228–244, 2016. DOI: 10.1016/j.ymssp.2015.12.015.

[7] P. S. Wright. Short-time Fourier transforms and Wigner-Ville distributions applied to the calibration of power frequency harmonic analyzers. *IEEE Transactions on Instrumentation and Measurement*, vol. 48, no. 2, pp. 475–478, 1999. DOI: 10.1109/19.769633.

[8] J. H. Lee, J. Kim, H. J. Kim. Development of enhanced Wigner-Ville distribution function. *Mechanical Systems and Signal Processing*, vol. 15, no. 2, pp. 367–398, 2001. DOI: 10.1006/mssp.2000.1365.

[9] A. R. B. Abdullah, A. Z. B. Sha'ameri, B. J. Auzani. Classification of power quality signals using smooth-windowed Wigner-Ville distribution. In *Proceedings of International Conference on Electrical Machines and Systems*, IEEE, Incheon, South Korea, pp. 1981–1985, 2010.

[10] H. He, J. A. Starzyk. A self-organizing learning array system for power quality classification based on wavelet transform. *IEEE Transactions on Power Delivery*, vol. 21, no. 1, pp. 286–295, 2006. DOI: 10.1109/TPWRD.2005.852392.

[11] S. Santoso, W. M. Grady, E. J. Powers, J. Lamoree, S. C. Bhatt. Characterization of distribution power quality events with Fourier and wavelet transforms. *IEEE Transactions on Power Delivery*, vol. 15, no. 1, pp. 247–254, 2000. DOI: 10.1109/61.847259.

[12] R. Q. Yan, R. X. Gao, X. F. Chen. Wavelets for fault diagnosis of rotary machines: A review with applications. *Signal Processing*, vol. 96, pp. 1–15, 2014. DOI: 10.1016/j.sigpro.2013.04.015.

[13] D. De Yong, S. Bhowmik, F. Magnago. An effective power quality classifier using wavelet transform and support vector machines. *Expert Systems with Applications*, vol. 42, no. 15–16, pp. 6075–6081, 2015. DOI: 10.1016/j.eswa.2015.04.002.

[14] Z. K. Peng, P. W. Tse, F. L. Chu. An improved Hilbert-Huang transform and its application in vibration signal analysis. *Journal of Sound and Vibration*, vol. 286, no. 1–2, pp. 187–205, 2005. DOI: 10.1016/j.jsv.2004.10.005.

[15] J. H. Yan, L. Lu. Improved Hilbert-Huang transform based weak signal detection methodology and its application on incipient fault diagnosis and ECG signal analysis. *Signal Processing*, vol. 98, pp. 74–87, 2014. DOI: 10.1016/j.sigpro.2013.11.012.

[16] P. K. Dash, B. K. Panigrahi, G. Panda. Power quality analysis using S-transform. *IEEE Transactions on Power Delivery*, vol. 18, no. 2, pp. 406–411, 2003. DOI: 10.1109/TPWRD.2003.809616.

[17] P. K. Dash, B. K. Panigrahi, D. K. Sahoo, G. Panda. Power quality disturbance data compression, detection, and classification using integrated spline wavelet and S-transform. *IEEE Transactions on Power Delivery*, vol. 18, no. 2, pp. 595–600, 2003. DOI: 10.1109/TPWRD.2002.803824.

[18] O. P. Mahela, A. G. Shaik. Recognition of power quality disturbances using S-transform based ruled decision tree and fuzzy C-means clustering classifiers. *Applied Soft Computing*, vol. 59, pp. 243–257, 2017. DOI: 10.1016/j.asoc.2017.05.061.

[19] R. Kumar, B. Singh, D. T. Shahani, A. Chandra, K. Al-Haddad. Recognition of power-quality disturbances using S-transform-based ANN classifier and rule-based decision tree. *IEEE Transactions on Industry Applications*, vol. 51, no. 2, pp. 1249–1258, 2015. DOI: 10.1109/TIA.2014.2356639.

[20] O. P. Mahela, A. G. Shaik, N. Gupta. A critical review of detection and classification of power quality events. *Renewable and Sustainable Energy Reviews*, vol. 41, pp. 495–505, 2015. DOI: 10.1016/j.rser.2014.08.070.

[21] H. S. Behera, P. K. Dash, B. Biswal. Power quality time series data mining using S-transform and fuzzy expert system. *Applied Soft Computing*, vol. 10, no. 3, pp. 945–955, 2010. DOI: 10.1016/j.asoc.2009.10.013.

[22] J. B. V. Reddy, P. K. Dash, R. Samantaray, A. K. Moharana. Fast tracking of power quality disturbance signals using an optimized unscented filter. *IEEE Transactions on Instrumentation and Measurement*, vol. 58, no. 12, pp. 3943–3952, 2009. DOI: 10.1109/TIM.2009.2020835.

[23] X. Ouyang, M. G. Amin. Short-time Fourier transform receiver for nonstationary interference excision in direct sequence spread spectrum communications. *IEEE Transactions on Signal Processing*, vol. 49, no. 4, pp. 851–863, 2001. DOI: 10.1109/78.912929.

[24] M. Analysis of nonstationary power-quality waveforms using iterative Hilbert Huang transform and SAX algorithm. *IEEE Transactions on Power Delivery*, vol. 28, no. 4, pp. 2134–2144, 2013. DOI: 10.1109/TPWRD.2013.2264948.

[25] Y. Huang, Y. Q. Liu, Z. P. Hong. Detection and location of power quality disturbances based on mathematical morphology and Hilbert-Huang transform. In *Proceedings of the 9th International Conference on Electronic Measurement & Instruments*, IEEE, Beijing, China, 2000. DOI: 10.1109/ICEMI.2009.5274596.

[26] S. Santoso, E. J. Powers, W. M. Grady, A. C. Parsons. Power quality disturbance waveform recognition using wavelet-based neural classifier. I. Theoretical foundation. *IEEE Transactions on Power Delivery*, vol. 15, no. 1, pp. 222–228, 2000. DOI: 10.1109/61.847255.

[27] M. Biswal, P. K. Dash. Detection and characterization of multiple power quality disturbances with a fast S-transform and decision tree based classifier. *Digital Signal Processing*, vol. 23, no. 4, pp. 1071–1083, 2013. DOI: 10.1016/j.dsp.2013.02.012.

[28] P. K. Dash, S. Das, J. Moirangthem. Distance protection of shunt compensated transmission line using a sparse S-transform. *IET Generation, Transmission & Distribution*, vol. 9, no. 12, pp. 1264–1274, 2015. DOI: 10.1049/iet-gtd.2014.1002.

[29] M. V. Chilukuri, P. K. Dash. Multiresolution S-transform-based fuzzy recognition system for power quality events. *IEEE Transactions on Power Delivery*, vol. 19, no. 1, pp. 323–330, 2004. DOI: 10.1109/TPWRD.2003.820180.

[30] R. A. Brown, R. Frayne. A fast discrete S-transform for biomedical signal processing. In *Proceedings of the 30th Annual International Conference of IEEE Engineering in Medicine and Biology Society*, IEEE, Vancouver, Canada, pp. 2586–2589, 2008. DOI: 10.1109/IEMBS.2008.4649729.

[31] R. A. Brown, M. L. Lauzon, R. Frayne. A general description of linear time-frequency transforms and formulation of a fast, invertible transform that samples the continuous S-transform spectrum nonredundantly. *IEEE Transactions on Signal Processing*, vol. 58, no. 1, pp. 281–290, 2010. DOI: 10.1109/TSP.2009.2028972.

[32] C. Cortes, V. Vapnik. Support-vector networks. *Machine Learning*, vol. 20, no. 3, pp. 273–297, 1995. DOI: 10.1007/BF00994018.

[33] J. A. K. Suykens, J. Vandewalle. Least squares support vector machine classifiers. *Neural Processing Letters*, vol. 9, no. 3, pp. 293–300, 1999. DOI: 10.1023/A:1018628609742.

[34] P. Cross, X. D. Ma. Model-based and fuzzy logic approaches to condition monitoring of operational wind turbines. *International Journal of Automation and Computing*, vol. 12, no. 1, pp. 25–34, 2015. DOI: 10.1007/s11633-014-0863-9.

[35] B. Biswal, P. K. Dash, B. K. Panigrahi. Power quality disturbance classification using fuzzy C-means algorithm and adaptive particle swarm optimization. *IEEE Transactions on Industrial Electronics*, vol. 56, no. 1, pp. 212–220, 2009. DOI: 10.1109/TIE.2008.928111.

[36] F. Hoffmann. Combining boosting and evolutionary algorithms for learning of fuzzy classification rules. *Fuzzy Sets and Systems*, vol. 141, no. 1, pp. 47–58, 2004. DOI: 10.1016/S0165-0114(03)00113-1.

[37] M. Seera, C. P. Lim, C. K. Loo, H. Singh. Power quality analysis using a hybrid model of the fuzzy min-max neural network and clustering tree. *IEEE Transactions on Neural Networks and Learning Systems*, vol. 27, no. 12, pp. 2760–2767, 2016. DOI: 10.1109/TNNLS.2015.2502955.

[38] S. Khokhar, A. Asuhaimi B. Mohd Zin, A. S. B. Mokhtar, M. Pesaran. A comprehensive overview on signal processing and artificial intelligence techniques applications in classification of power quality disturbances. *Renewable and Sustainable Energy Reviews*, vol. 51, pp. 1650–1663, 2015. DOI: 10.1016/j.rser.2015.07.068.

[39] S. Chakravarty, P. K. Dash. A PSO based integrated functional link net and interval type-2 fuzzy logic system for predicting stock market indices. *Applied Soft Computing*, vol. 12, no. 2, pp. 931–941, 2012. DOI: 10.1016/j.asoc.2011.09.013.

[40] Y. Wang, X. X. Zhu. A robust design of hybrid fuzzy controller with fuzzy decision tree for autonomous intelligent parking system. In *Proceedings of American Control Conference*, IEEE, Portland, USA, 2014. DOI: 10.1109/ACC.2014.6859439.

[41] Y. Wang, X. X. Zhu. Hybrid fuzzy logic controller for optimized autonomous parking. In *Proceedings of American Control Conference*, IEEE, Washington DC, USA, 2013. DOI: 10.1109/ACC.2013.6579834.

[42] Y. Wang, X. X. Zhu. Design and implementation of an integrated multi-functional autonomous parking system with fuzzy logic controller. In *Proceedings of American Control Conference*, IEEE, Montreal, Canada, 2012. DOI: 10.1109/ACC.2012.6315356.

[43] S. R. Safavian, D. Landgrebe. A survey of decision tree classifier methodology. *IEEE Transactions on Systems, Man, and Cybernetics*, vol. 21, no. 3, pp. 660–674, 1991. DOI: 10.1109/21.97458.

[44] C. X. Dou, T. Gui, Y. F. Bi, J. Z. Yang, X. G. Li. Assessment of power quality based on D-S evidence theory. *International Journal of Automation and Computing*, vol. 11, no. 6, pp. 635–643, 2014. DOI: 10.1007/s11633-014-0837-y.

[45] L. F. Mendonca, S. M. Vieira, J. M. C. Sousa. Decision tree search methods in fuzzy modeling and classification. *International Journal of Approximate Reasoning*, vol. 44, no. 2, pp. 106–123, 2007. DOI: 10.1016/j.ijar.2006.07.004.

[46] C. Z. Janikow. Fuzzy decision trees: Issues and methods. *IEEE Transactions on Systems, Man, and Cybernetics, Part B* (*Cybernetics*), vol. 28, no. 1, pp. 1–14, 1998. DOI: 10.1109/3477.658573.

[47] R. Chassaing. *Digital Signal Processing and Applications with the C6713 and C6416 DSK*, Hoboken, USA: John Wiley & Sons, 2004.

N. R. Nayak received the B. Eng. in electronics and telecommunication from Utkal University, India in 1992, the M. Eng. degree in communication system engineering from Biju Patnaik University of Technology, India in 2004, and the Ph. D. degree from Siksha "O" Anusandhan University, India in 2017. He is currently the director of Microsys Infotech, India.

His research interests include signal processing, pattern recognition and classification.

E-mail: nihar.microsys@gmail.com

ORCID iD: 0000-0002-1524-7837

P. K. Dash received the M. Eng. degree in electrical engineering from Indian Institute of Science, India in 1964, the Ph. D. degree in electrical engineering from the Sambalpur University, India in 1972, and the D. Sc. degree in electrical engineering from the Utkal University, India in 2003. He is currently director of research in the Multidisciplinary Research Cell of the Siksha "O" Anusandhan University, India. He has published more than 500 papers in international journals and conferences.

His research interests include renewable energy, micro and smart grid, machine intelligence, signal processing and control, power quality.

E-mail: pkdash.india@gmail.com (Corresponding author)

ORCID iD: 0000-0002-8950-7136

R. Bisoi received the M. Eng. degree in computer application from North Orissa University, India in 2011, and the Ph. D. degrees in computer engineering from Siksha "O" anusandhan University, India 2015. She is currently working as a research officer in the Multidisciplinary Research Cell of Siksha "O" Anusandhan University, India. She has published 25 papers in international journals and conferences.

Her research interests include computing software, data mining, machine intelligence and bioinformatics.

E-mail: ranjeeta.bisoi@gmail.com

ORCID iD: 0000-0002-2651-2130